




RESEARCH ARTICLE

Regional structural hypo- and hyperconnectivity of frontal–striatal and frontal–thalamic pathways in behavioral variant frontotemporal dementia

David Jakabek¹  | Brian D. Power² | Matthew D. Macfarlane^{1,3} |
 Mark Walterfang⁴ | Dennis Velakoulis⁴ | Danielle van Westen⁵ | Jimmy Lätt^{5,6} |
 Markus Nilsson⁶  | Jeffrey C. L. Looi^{4,7}  | Alexander F. Santillo⁸

¹Graduate School of Medicine, University of Wollongong, Wollongong, Australia

²School of Medicine, The University of Notre Dame Australia, Fremantle, Australia; Clinical Research Centre, North Metropolitan Health Service - Mental Health, Perth, Australia

³Illawarra Shoalhaven Local Health District, Wollongong, Australia

⁴Neuropsychiatry Unit, Royal Melbourne Hospital, Melbourne Neuropsychiatry Centre, Department of Psychiatry, Melbourne Medical School, University of Melbourne, Melbourne, Australia

⁵Centre for Medical Imaging and Physiology, Skåne University Hospital, Lund, Sweden

⁶Department of Radiology, Department of Clinical Sciences Lund, Lund University, Lund, Sweden

⁷Research Centre for the Neurosciences of Ageing, Academic Unit of Psychiatry and Addiction Medicine, Australian National University Medical School, Canberra Hospital, Canberra, Australia

⁸Clinical Memory Research Unit, Department of Clinical Sciences, Lund University, Lund, Sweden

Correspondence

Dr David Jakabek, c/o School of Medicine, Building 28, University of Wollongong, Northfields Avenue, Wollongong NSW 2522, Australia.
 Email: djakabek@gmail.com

Funding information

Miller Family Bridgewater Illawarra Health and Medical Research Initiative Summer Scholarship; The Swedish Alzheimer foundation; Thuréus foundation; The Swedish Society for Medical Research; The Bente Rexed Gersteds Foundation for Brain Research

Abstract

Behavioral variant frontotemporal dementia (bvFTD) has been predominantly considered as a fronto-temporal cortical disease, with limited direct investigation of frontal–subcortical connections. We aim to characterize the grey and white matter components of frontal–thalamic and frontal–striatal circuits in bvFTD. Twenty-four patients with bvFTD and 24 healthy controls underwent morphological and diffusion imaging. Subcortical structures were manually segmented according to published protocols. Probabilistic pathways were reconstructed separately from the dorsolateral, orbitofrontal and medial prefrontal cortex to the striatum and thalamus. Patients with bvFTD had smaller cortical and subcortical volumes, lower fractional anisotropy, and higher mean diffusivity metrics, which is consistent with disruptions in frontal–striatal–thalamic pathways. Unexpectedly, regional volumes of the striatum and thalamus connected to the medial prefrontal cortex were significantly larger in bvFTD (by 135% in the striatum, $p = .032$, and 217% in the thalamus, $p = .004$), despite smaller dorsolateral prefrontal cortex connected regional volumes (by 67% in the striatum, $p = .002$, and 65% in the thalamus, $p = .020$), and inconsistent changes in orbitofrontal cortex connected regions. These unanticipated findings may represent compensatory or maladaptive remodeling in bvFTD networks. Comparisons are made to other neuropsychiatric disorders suggesting a common mechanism of changes in frontal–subcortical networks; however, longitudinal studies are necessary to test this hypothesis.

KEYWORDS

behavioral variant frontotemporal dementia, connectivity, DTI, MRI, probabilistic tractography

Jeffrey C. L. Looi and Alexander F. Santillo contributed equally to this work.

Stat rosa pristina nomine, nomina nuda tenemus –

“Yesterday’s rose stands only in its name, we hold only empty names”

The Name of the Rose - Umberto Eco

1 | INTRODUCTION

Behavioral variant frontotemporal dementia (bvFTD) is the most common frontotemporal dementia subtype, with deficits in executive functioning, social cognition, and alterations to behavior (Piguet, Hornberger, Mioshi, & Hodges, 2011). Although frontal and temporal cortical lobar degeneration is a defining and diagnostic criterion of the disease (Rascovsky et al., 2011), atrophy of the caudate, putamen, and thalamus is also well described (Chow et al., 2008; Garibotto et al., 2011; Gordon, Rohrer, & Fox, 2016; Halabi et al., 2013; Landin-Romero et al., 2016; Looi et al., 2008, 2009; O’Callaghan, Bertoux, & Hornberger, 2014). Given this degeneration across nodes in frontal-striatal-thalamic circuits (Alexander, DeLong, & Strick, 1986), bvFTD has progressively been recast as a disorder of cortical-subcortical circuits, rather than isolated cortical disease alone (Bertoux, O’Callaghan, Flanagan, Hodges, & Hornberger, 2015; Looi et al., 2012; Schroeter, Raczka, Neumann, & von Cramon, 2008; Schroeter et al., 2014; Seeley, Crawford, Zhou, Miller, & Greicius, 2009).

Frontal-striatal and frontal-thalamic circuits are well described in healthy populations and have associations with behavioral alterations in disease. Frontal-striatal tracts have been segmented with both structural (Draganski et al., 2008) and functional (Choi, Yeo, & Buckner, 2012) imaging, with separate divisions of these tracts demonstrated depending on their cortical origin. Striatal and thalamic terminations of these tracts can be mapped in a topographic manner in both exclusive (Draganski et al., 2008) and overlapping (Jarbo & Verstynen, 2015) regions. Similarly, frontal-thalamic tracts can also be divided based on cortical origin (Klein et al., 2010) and terminate in different regions of the thalamus (Behrens et al., 2003; Jang & Yeo, 2014). These frontal subcortical structural connections are implicated in varied neurodegenerative disease processes. Although the frontal cortex is implicated in execution of goal-directed behavior (Piray, Toni, & Cools, 2016), breakdown in either subcortical nodes or the frontal-subcortical connections is associated with similar behavioral deficits (Bhatia & Marsden, 1994). Thus, our interest expands to the different subdivisions of frontal-striatal and frontal-thalamic pathways.

Despite the established cortical effects of bvFTD and the known topographical correspondence between cortical and subcortical structures, the cortical-subcortical connectivity in bvFTD is incompletely investigated. A voxel based morphometry study examined indirect cortical-striatal connectivity and found correlated atrophy between frontal regions (ventromedial and dorsolateral prefrontal cortex) and connected striatal regions (Bertoux et al., 2015) using atlas-based divisions of the striatum. However, this atlas-based measure may not distinguish between different frontal-striatal divisions. Similarly, our previous striatal morphology analysis in bvFTD demonstrated striatal atrophy predominantly in anterior regions of the caudate (Macfarlane et al., 2015).

These regions connect to the prefrontal cortex, and thus also provide indirect structural evidence of localized node atrophy in frontal-striatal pathways. Nevertheless, direct examination of structural white matter pathways between the frontal cortex and striatum in bvFTD is lacking. The white matter microstructure of frontal-thalamic connections has been explored with diffusion tensor imaging (DTI), with bvFTD patients demonstrating lower fractional anisotropy (FA), and higher axial diffusivity (AD), radial diffusivity (RD) and mean diffusivity (MD) (Daianu et al., 2016; Mahoney et al., 2014; Möller et al., 2015; Zhang et al., 2009). However, quantification of the metrics across different divisions of the anterior thalamic radiation has not been explored. Lastly, evidence from functional imaging in bvFTD is conflicting. Zhou et al. (2010) found increased default mode network activity, yet decreased Salience Network activation between the cortex, putamen, and thalamus. More recently Farb et al. (2013) reported increased functional activity between the medial prefrontal cortex and the striatum. In summary, there is fragmentary evidence of altered frontal-striatal and frontal-thalamic pathway integrity and functioning in bvFTD, although the integrity of these pathways has not been sufficiently investigated.

The aim of this study is to comprehensively describe the structural frontal-striatal and frontal-thalamic pathways in bvFTD at an individual level by using probabilistic tractography. We hypothesize that bvFTD patients, compared to controls, will (a) have impaired white matter microstructure, as measured via diffusion tensor imaging metrics, in frontal-striatal and frontal-thalamic pathways; (b) exhibit atrophy of regions of the striatum and thalamus which connect to prefrontal areas; and (c) these imaging findings are associated with clinical and behavioral measures.

2 | MATERIAL AND METHODS

2.1 | Participants

Participants were from the Lund Prospective Frontotemporal Dementia Study, a longitudinal study of patients with any of the frontotemporal dementia spectrum disorders. We used data collected at the baseline for this study. Clinical work up included a clinical examination, neuropsychological examination, structured caregiver interview (see below), MRI, and cerebrospinal fluid analysis. Behavioral variant frontotemporal lobe degeneration consensus criteria (Rascovsky et al., 2011) were used for diagnosis at diagnostic conference (six definitive, 18 probable). Cerebrospinal fluid biomarkers consistent with Alzheimer’s disease (Blennow, Hampel, Weiner, & Zetterberg, 2010) were used as exclusion criteria. Healthy controls underwent the same procedures as the patients, and showed no signs of neurological or psychiatric conditions. Participants included some from previously published works on this cohort (Macfarlane et al., 2015; Santillo et al., 2013, 2016) where valid MRI data was available.

Informed consent was obtained from participants. However, if any doubt over capacity for consent was present, then consent was also sought from the participant’s primary caregiver. In all cases, participants could cease participation at any time. Ethics approval was granted by Regional Ethical Review Board, Lund, Sweden. Ethics approval for the

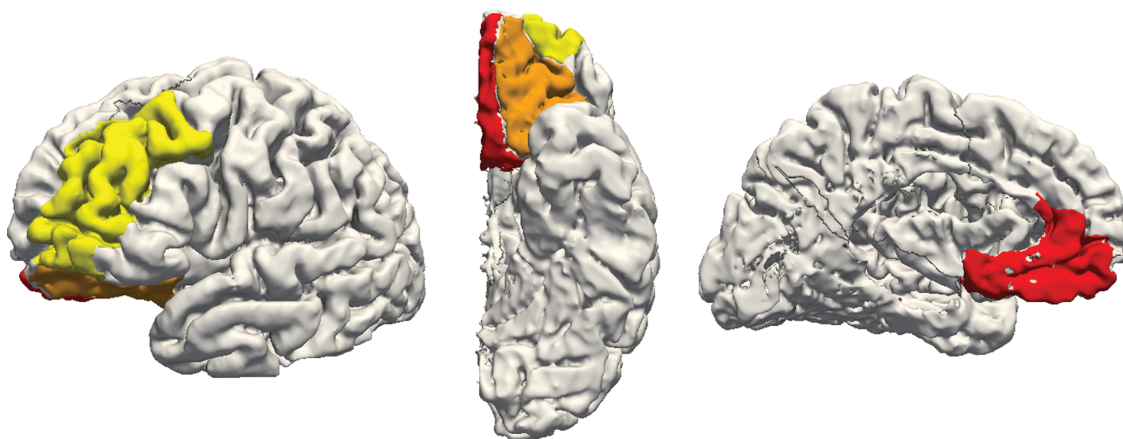


FIGURE 1 Cortical regions extracted from Freesurfer ROIs for a sample participant's left hemisphere, showing lateral (left), inferior (middle), and medial (right) views. Regions selected are the dorsolateral prefrontal cortex (yellow), medial prefrontal cortex (red), and orbitofrontal cortex (orange) [Color figure can be viewed at wileyonlinelibrary.com]

analysis via the Australian National University Medical School was granted by the Australian National University Human Research Ethics Committee.

2.2 | Behavioral assessment

Disease severity was rated by an experienced clinician based on an interview with the patients' primary caregiver using the Frontotemporal Lobar Degeneration modified Clinical Dementia Rating Scale (Knopman et al., 2008), which assess cognitive and global functioning, including behavior, and language. We utilized the sum of boxes (FTLD-CDR-SB) score as a continuous variable in analyses. Additionally, behavioral disturbance was assessed in the same interview using the Frontal Behavioral Inventory (FBI; Kertesz, Davidson, & Fox, 1997), a 24-item rating scale capturing a broad range of prefrontal syndrome behavior, the total sum of which was used in this study.

2.3 | Image acquisition

A Philips Achieva 3 T scanner with an eight-channel head coil was used for all acquisitions. T1 images used an MPRAGE sequence with TR = 8.3 ms, TE 3.84 ms, FOV = 256 × 256 × 175 mm³ and 1 mm³ isotropic voxels. FLAIR sequences were utilized to examine for cerebrovascular lesions by a senior neuroradiologist. DTI sequences were obtained in transverse slice orientation using a single-shot echo planar imaging sequence (TR = 7,881 ms, TE = 90 ms) with 48 encoding directions (one $b = 0$ and 48 $b = 800$ s/mm² volumes) using 2 mm isotropic voxels in 50 slices.

2.4 | Image processing

T1 scans were parcellated using Freesurfer 5.3 software (<http://surfer.nmr.mgh.harvard.edu>). Reconstructions were examined and manually corrected by DJ as per the troubleshooting guide, predominantly for excess inclusion of grey matter in dural sinuses. Cortical masks were extracted based on parcellation regions of interest (ROI) using the Desikan-Killiany atlas (Desikan et al., 2006) and are displayed in Figure 1.

We utilized ROIs as defined by Petrides and Pandya (2002) and Draganski et al. (2008) by extracting the DLPFC (from the rostral middle frontal ROI), MPFC (combined rostral anterior cingulate and medial orbitofrontal ROIs), and OFC (lateral orbital frontal ROI). The estimated total intracranial volume measure was utilized to normalize for head size.

Striatal and thalamic volumes were manually defined using established protocols with excellent reliability. The caudate (Looi et al., 2008) and putamen (Looi et al., 2009) were segmented separately in ITK-SNAP software (Yushkevich et al., 2006). We used the combined segmentation of the caudate and putamen for subsequent analyses as their connectivity and function are closely related (Draganski et al., 2008). Thalamic segmentations were performed using ANALYZE software (Mayo Biomedical Imaging Resource, Rochester, MN) using T1 sequences (and inversed T1 images) to delineate the boundaries (Power et al., 2015).

Volume registration was performed to correct for eddy current distortion using FSL `eddy_correct` script (Smith et al., 2004; Woolrich et al., 2009), and b vectors rotated accordingly (Leemans & Jones, 2009). Diffusion maps (FA, AD, RD, and MD) were created with FSL DTIFIT package.

Nonlinear registration was performed between structural, diffusion, and standard space images using FSL FNIRT tool (Andersson, Jenkinson, & Smith, 2012). The T1 images were registered to diffusion images, acquired with $b = 0$ s/mm², using nonlinear registration to account for distortions in the echo planar imaging volumes. Additionally, T1 images were registered to standard MNI152 images also using nonlinear registration to account for increased ventricle size in bvFTD participants. These transforms were inverted and concatenated to transform images between spaces. Segmentations transformed to MNI space were manually checked for accuracy.

2.5 | Tractography

Probabilistic tractography was performed within each participant's diffusion space. For each target structure (striatum and thalamus), we

TABLE 1 Participant characteristics

Demographics	Control		bvFTD		<i>p</i> value
<i>n</i>	24		24		
Male	13		11		.564
	<i>M</i>	<i>SD</i>	<i>M</i>	<i>SD</i>	
Age	66.0	11.6	68.6	8.5	.017
Education (years)	11.6	2.7	9.6	2.6	.009
eTICV (voxels × 10 ⁴)	15.1	1.4	14.5	9.9	.168
MMSE	29.5	0.5	23.5	4.6	<.001
FTLD-CDR-SB			8.8	3.7	
FBI Total			26.8	8.3	

Note. Abbreviations: bvFTD = behavioral variant frontotemporal dementia; eTICV = estimated total intracranial volume; FBI = frontal behavior inventory total score; FTLD-CDR-SB = frontotemporal lobar degeneration modified clinical dementia rating scale sum of boxes; MMSE = Mini-Mental State Examination.

Significant statistical difference was assessed using Chi-squared test for gender and independent *t* tests for other variables.

generated streamline probability distribution maps from each frontal region (DLPFC, MPFC, and OFC). In each map the frontal region was specified as seed, striatum or thalamus as target, and contralateral white matter as exclusion mask. Frontal regions and subcortical segmentations were obtained by transforming them from standard and structural space, respectively, into diffusion space using previously generated registrations.

For computation of DTI metrics of pathways, we adapted the methodology of Nakamae et al. (2014). Briefly, probabilistic tractography was performed using BedpostX (Jbabdi, Woolrich, Andersson, & Behrens, 2007) with default parameters. Pathway probability maps were normalized for seed size by dividing the probability maps by the total number of successfully generated streamlines (the "waytotal"), and spurious connections were removed by thresholding the resulting maps by 10%. Thresholded probability maps were then binarized and overlaid on DTI metric maps (FA, AD, RD, and MD) from which average values were extracted.

For analysis of subcortical regional volumes, we used diffusion target classification (as in Behrens et al., 2003). That is, probabilistic tractography was carried out between frontal seeds and striatal and thalamic targets, separately. This allowed us to determine which areas within the striatum and thalamus were predominantly connected to which frontal area. To remove false-positives, we thresholded the connectivity maps by the top 10% (as in Bohanna, Georgiou-Karistianis, & Egan, 2011) before calculating the final volume. We also conducted analyses with threshold levels of 5% and 20% with similar findings.

2.6 | Statistical analysis

Statistical analyses were performed in SPSS 23.0 (IBM Corp. Released 2015. IBM SPSS Statistics for Windows, Version 23.0. Armonk, NY: IBM Corp.). Demographic measures were compared with an independent *t* test, Mann-Whitney *U* test, or Chi-squared tests as appropriate.

Mixed models were utilized for all subsequent analyses, with hemisphere treated as a repeated factor to examine for structural asymmetry. In all analyses, age, gender, and years of education were standardized and included as covariates. For volumetric analyses, we utilized estimated total intracranial volume as a covariate to normalize for brain volume.

Assumptions of normality were upheld for all diffusion indices, DLPFC-striatum and DLPFC-thalamus connected volumes. Other volumes were significantly (Kolmogorov-Smirnov test <0.05) right skewed. Thus, we utilized linear mixed models for normally distributed variables and generalized mixed models with a Gamma distribution and log-linked function for the remainder. Models were specified with random intercepts. Hemisphere was included as a repeated factor considering possible lateralization in bvFTD (Gordon et al., 2016) and to reduce the number of comparisons, thus allowing us to test for abnormal lateralization utilizing a group-by-hemisphere interaction term. We calculated an effect size measure comparable to Cohen's *d* using the difference between estimated marginal means proportional to the estimated standard deviation of control participants.

DTI metrics and volumes were compared between groups with statistical significance considered when *p* < .05. For bvFTD patients only, we specified models which predicted DTI metrics or volumes based on FTLD-CDR-SB measure and FBI total score predictors using mixed models. Due to the number of comparisons with these behavioral tests, we used a more stringent *p* value of .004 (.05 divided by four different measures for three different pathways).

3 | RESULTS

3.1 | Participants

A total of 54 participants were recruited for this study; however, six patients were excluded (three due to no DTI data; one each due to excessive motion during scanning, severe echo planar imaging distortions, and inadvertent exclusion of a portion of the brain from the T1W volume). One patient had a small lacunar infarct in the right putamen;

TABLE 2 Group differences in number of voxels between frontal and subcortical volumes

Structure	Control		bvFTD		<i>p</i> value	Effect size
	<i>M</i>	<i>SD</i>	<i>M</i>	<i>SD</i>		
DLPFC	14,054	1,521	11,759	1,487	<.001	1.53
MPFC	3,359	407	2,786	398	<.001	1.42
OFC	6,508	837	5,380	819	<.001	1.36
Striatum	5,286	655	5,201	652	<.001	0.13
Thalamus	4,555	612	4,138	586	.029	0.70

Note. Abbreviations: bvFTD = behavioral variant frontotemporal dementia; DLPFC = dorsolateral prefrontal cortex; MPFC = medial prefrontal cortex; OFC = orbitofrontal cortex. Estimated marginal mean voxels and significance test from separate linear mixed models, controlling for hemisphere, age, gender, education, and intracranial volume.

however, given the aggregation of striatal structures, this participant was included in subsequent analyses. Demographic details of included participants are provided in Table 1.

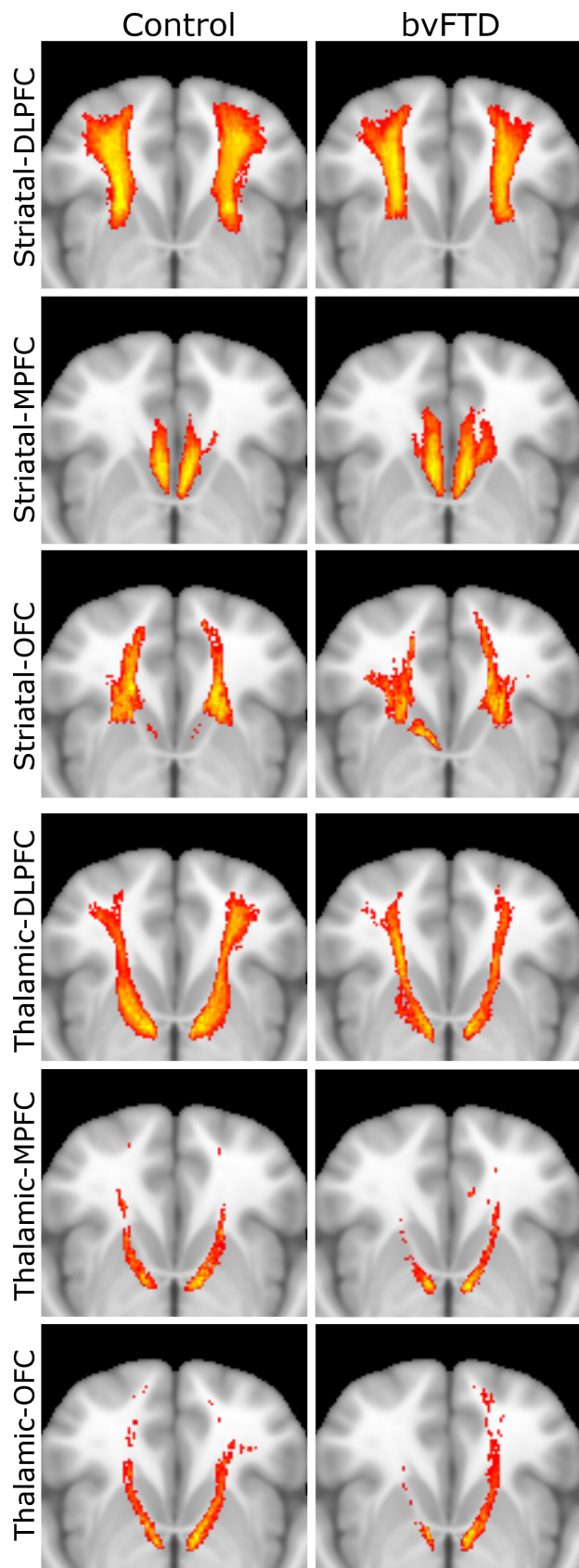


FIGURE 2

3.2 | Comparison of cortical and subcortical volumes

Smaller volumes were observed in patients compared with controls for both cortical regions and subcortical structures (Table 2). There were no significant group-by-hemisphere interaction effects.

3.3 | Frontal-striatal and frontal-thalamic connectivity

The frontal-striatal and frontal-thalamic streamlines are visualized in Figure 2. There was a clear inferior-superior gradient between tracts, with tracts from the OFC running lower than MPFC tracts, MPFC tracts sitting more medially, and DLPFC tracts taking a more superior and lateral course. Frontal-striatal streamlines were successfully generated for all participants and regions. Frontal-thalamic tracts streamlines could not be generated for from the MPFC in the right hemisphere in one bvFTD patient, and five tracts from the OFC (two each from bvFTD patients in each hemisphere, one in a control participant's left hemisphere).

Diffusion tensor imaging metrics between tracts generally differed between groups for both frontal-striatal tracts (Table 3) and frontal-thalamic tracts (Table 4). Decreased FA, and increased AD, RD, and MD were noted across all tracts and indices. No group-by-hemisphere interactions were statistically significant.

3.4 | Striatal and thalamic connectivity parcellation and volumetrics

Thalamic and striatal connectivity maps in patients and controls are displayed in Figure 3 and volumetrics are compared between groups in Table 5. The size of DLPFC connected regions decreased in bvFTD while MPFC connected regions increased in volume in bvFTD patients compared to controls. OFC connection volumes were significantly decreased in the striatum and nonstatistically significantly increased in the thalamus. There was no significant group-by-hemisphere effect.

3.5 | Associations with behavioral measures

There were few significant associations of behavioral measures with prefrontal areas, subcortical structures, diffusion indices or regional volumes. All results are presented in Supporting Information, Table 1. Significant findings at a revised statistical threshold of $p < .004$ were present for the total OFC volume with FTLD-CDR-SB scale (unstandardized $B = -179.472$, $p = .003$). Significant diffusion associations were present between the FDR-CDR sum of boxes scale and DLPFC-striatal

FIGURE 2 Frontal-striatal (top three rows) and frontal-thalamic (bottom three rows) pathways in controls (left column) and bvFTD participants (right column). Horizontal view of pathways aligned to MNI152 space and superimposed on standard MNI152 brain. Colors reflect extent of overlap between participants, with red indicating at least 50% overlap and yellow indicating 100%. bvFTD = behavioral variant frontotemporal dementia; DLPFC = dorsolateral prefrontal cortex; MPFC = medial prefrontal cortex; OFC = orbitofrontal cortex [Color figure can be viewed at wileyonlinelibrary.com]

TABLE 3 DTI metrics for frontal–striatal pathways

Cortical seed	Control		bvFTD		<i>p</i> value	Effect size
	<i>M</i>	<i>SD</i>	<i>M</i>	<i>SD</i>		
DLPFC						
FA	0.36	0.17	0.29	0.17	<.001	0.38
AD	1.19	0.83	1.34	0.08	<.001	0.27
RD	0.69	0.08	0.88	0.08	<.001	2.25
MD	0.86	0.08	1.03	0.08	<.001	2.13
MPFC						
FA	0.27	0.03	0.24	0.03	<.001	1.09
AD	1.29	0.69	1.40	0.69	.008	0.16
RD	0.89	0.50	1.01	0.50	.002	0.24
MD	1.03	1.24	1.14	1.24	.003	0.09
OFC						
FA	0.34	0.17	0.29	0.17	<.001	0.31
AD	1.21	0.08	1.31	0.07	<.001	1.37
RD	0.73	0.43	0.87	0.43	<.001	0.33
MD	0.89	0.07	1.10	0.07	<.001	2.89

Note. Abbreviations: AD = apparent diffusivity; bvFTD = behavioral variant frontotemporal dementia; DLPFC = dorsolateral prefrontal cortex; FA = fractional anisotropy; MD = mean diffusivity; MPFC = medial prefrontal cortex; OFC = orbitofrontal cortex; RD = radial diffusivity. Estimated marginal mean DTI metrics (AD, RD, and MD all $\times 10^{-3}$) and significance tests from separate linear mixed models, controlling for hemisphere, age, gender, and education.

FA (unstandardized coefficient -0.028 , $p = .001$) and AD (unstandardized coefficient 0.076 , $p = .004$), and MPFC–striatal AD, RD, and MD (unstandardized coefficients, respectively, 0.111 , 0.106 , and 0.108 , $p = .001$ for all tests)

4 | DISCUSSION

In this study, we utilized individual probabilistic pathway reconstructions in a novel demonstration of altered frontal–striatal and frontal–thalamic connectivity in bvFTD. The key findings are the alteration of the frontal–striatal and frontal–thalamic white matter in bvFTD, and despite this, there is a selective increase of the MPFC connected regions in the striatum and thalamus. Our findings not only broaden the conceptual understanding of the specific neuro-pathophysiology of bvFTD, but may also illustrate neural circuit phenomena that may be common to frontal network system disorders.

We have demonstrated substantively altered white matter microstructure, as measured via diffusion tensor imaging metrics, for most divisions within the frontal–striatal and frontal–thalamic pathways. Fibers from the three frontal regions pass either directly to the striatum or within the anterior thalamic radiation to the thalamus. As a whole, altered white matter microstructure of the anterior thalamic radiation has been found in previous work (Daiyanu et al., 2016; Mahoney et al., 2014; Möller et al., 2015; Zhang et al., 2009). Moreover, we found that altered white matter microstructure, as measured via DTI metrics, was found in a similar magnitude and across all anatomical divisions in frontal–striatal projections, which to our knowledge, has yet to be empirically demonstrated in bvFTD. These frontal–striatal pathways involve predominantly cortical efferent projections, as opposed to the mixed

cortical–thalamic efferent and afferent projections within the anterior thalamic radiation. These findings may stem from direct neuropathological afflictions of white matter, which are present in the dominant bvFTD proteinopathies (i.e., tau and TDP-43) (Mackenzie & Neumann, 2016), or alternatively via direct and indirect deafferentation (i.e., downstream structural change in a brain region secondary to the interruption of afferent neuronal stimulation; Looi & Walterfang, 2013). Regardless of the pathological mechanisms, these findings highlight the importance of conceptualizing bvFTD as a dysfunction of cortical and subcortical transmission, in contrast to the prevailing cortico-cortical transmission focus.

Our gross volumetric findings reproduced the well-known atrophy of prefrontal and subcortical volumes in bvFTD (Chow et al., 2008; Garibotto et al., 2011; Gordon et al., 2016; Halabi et al., 2013; Landin-Romero et al., 2016; Looi et al., 2008, 2009; O'Callaghan et al., 2014). Our innovation is in demonstrating connectivity through the parcellation of striatal and thalamic regions which connect to prefrontal regions in bvFTD. As hypothesized, we demonstrate smaller DLPFC connected regions in the striatum and thalamus, and smaller OFC connected regions in the striatum only.

In contradistinction to the primarily atrophic changes, the regions of the striatum and thalamus which connect to the medial prefrontal cortex are significantly *increased* in size. This is despite a globalized decrease in volume, largely similar in magnitude, across all prefrontal and subcortical regions of interest in the bvFTD group (Table 2), and a similar degree of affliction of tracts generated from these regions (Tables 3 and 4). As explained more fully below, we chose to interpret this as structural hyperconnectivity, either as a primary pathological phenomenon, or more probably, as either compensatory or maladaptive phenomenon.

TABLE 4 DTI metrics for frontal–thalamic pathways

Cortical seed	Control		bvFTD		<i>p</i> value	Effect size
	<i>M</i>	<i>SD</i>	<i>M</i>	<i>SD</i>		
DLPFC						
FA	0.41	0.03	0.36	0.03	<.001	1.53
AD	1.20	0.41	1.34	0.41	<.001	0.33
RD	0.64	0.24	0.79	0.24	<.001	0.61
MD	0.83	0.07	0.97	0.06	<.001	2.19
MPFC						
FA	0.36	0.15	0.33	0.15	.002	0.20
AD	1.41	0.73	1.45	0.73	.369	0.06
RD	0.85	0.73	0.92	0.73	.119	0.09
MD	1.04	0.78	1.10	0.78	.180	0.07
OFC						
FA	0.39	0.03	0.33	0.03	<.001	1.60
AD	1.31	0.58	1.46	0.58	<.005	0.25
RD	0.76	0.45	0.93	0.45	<.001	0.38
MD	0.94	0.33	1.10	0.34	<.001	0.48

Note. Abbreviations: AD = apparent diffusivity; bvFTD = behavioral variant frontotemporal dementia; DLPFC = dorsolateral prefrontal cortex; FA = fractional anisotropy; MD = mean diffusivity; MPFC = medial prefrontal cortex; OFC = orbitofrontal cortex; RD = radial diffusivity. Estimated marginal mean DTI metrics (AD, RD, and MD all $\times 10^{-3}$) and significance tests from separate linear mixed models, controlling for hemisphere, age, gender, and education.

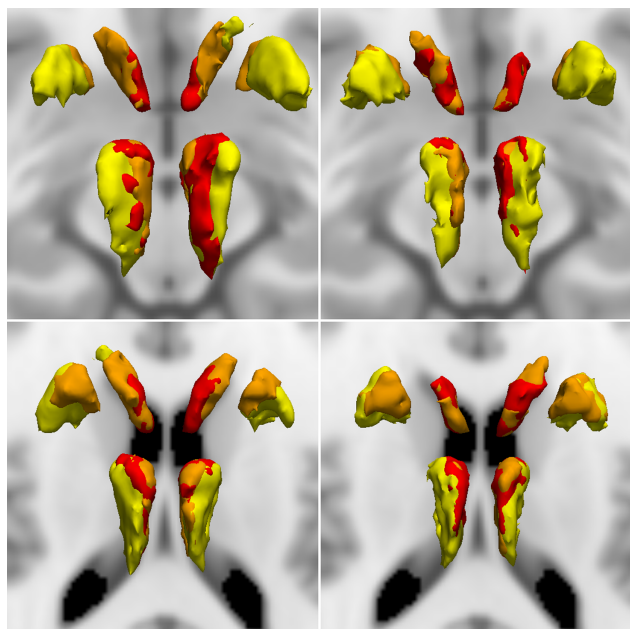


FIGURE 3 Parcellation of striatal and thalamic regions which connect to prefrontal seed regions, aligned to MNI152 space and superimposed on standard MNI152 brain. Top row, control participants; bottom row bvFTD participants; left column, superior views; right column, inferior views. Colors indicate cortical origin of streamlines as in Figure 1 (yellow, DLPFC; red, MPFC; orange, OFC). bvFTD = behavioral variant frontotemporal dementia. DLPFC = dorsolateral prefrontal cortex. MPFC = medial prefrontal cortex. OFC = orbitofrontal cortex [Color figure can be viewed at wileyonlinelibrary.com]

Our novel finding of increased volume in MPFC connected regions requires consideration of possible confounding factors. The recurrent frontal–striatal–thalamic–cortical circuitry is a structurally complex segregated parallel system which limits the extent in which it can be imaged in its full. The DLPFC pathways predominantly aggregate in the Muratoff bundle to the caudate, whereas the OFC and MPFC pathways predominantly traverse the external capsule to the putamen (Forkel et al., 2014; Schmahmann & Pandya, 2009). This corresponds with the pathways seen in Figure 2. For the frontal–thalamic connections we used, these proceed via the anterior thalamic radiation and our divisions match those previously published (Jang & Yeo, 2014). Thus, on visual inspection, these pathways are correctly specified. Moreover, our frontal connectivity-based parcellation of striatal and thalamic subregions is generally consistent with previous studies for both structures (Behrens et al., 2003; Draganski et al., 2008; Tziortzi et al., 2013), thus providing validation to our tractography methodology. Moreover, obtained DTI metrics are comparable to frontal probabilistic tractography in other conditions (Nakamae et al., 2014). Nevertheless, it should be noted that our parcellations in Figure 3 are not identical to previous studies due to the cortical regions (i.e., only the DLPFC, MPC, and OFC) we chose to utilize for this study. Thus, sensory, motor, and visual cortical regions are missing when compared to more comprehensive cortical parcellation schemes (Behrens et al., 2003; Draganski et al., 2008).

The other potential confounding factor for increased MFPC volume is the use of probabilistic tractography based on streamline propagation and diffusion tensor imaging (Jones & Cercignani, 2010). Increased volume in downstream regions may be attributed to increased streamline generation; however, we note that all frontal areas had a decrease in volume of equivalent magnitude in bvFTD (Table 2), thus leading to fewer streamline generation for all frontal regions. Nevertheless, we normalized all tracts by streamline counts. Additionally, streamline propagation may be paradoxically increased when these crossing fibers degenerate. However, all frontal–striatal and frontal–thalamic tracts course approximately orthogonally to the corpus callosum, the largest perpendicular interhemispheric fiber bundle. Moreover, change in the DTI metrics seen does not necessarily imply a larger reduction of crossing fibers in the MPFC generated tracts (Jones & Cercignani, 2010), as seen in Tables 2 and 3. Last, tract dispersion from pathway degeneration may explain our paradoxical findings, however since the rise in isotropy (as measures by RD and MD metrics) is larger in effect for DLPFC and OFC tracts rather than MPFC tracts, this is less likely. To confirm this, we would recommend future research employ specific measures of tract dispersion such as neurite orientation dispersion and density index (Zhang, Schneider, Wheeler-Kingshott, & Alexander, 2012) to characterize tracts further. Considered together, the isolated effect of increased volume of the MPFC connections, relatively lower isotropy of MPFC tracts, and the duplication of this effect in both the striatum and thalamus, suggests a reliable finding.

There is limited evidence of increased MPFC structural connectivity in other bvFTD literature. Our previous research in striatal morphology found paradoxical inflation of the head of the caudate in bvFTD patients (Macfarlane et al., 2015), although this was not observed in the anterior regions of the putamen. A voxel based morphometric analysis demonstrated opposite findings to our results, instead showing a positive correlation between atrophy of the ventromedian prefrontal cortex and connected striatal regions (Bertoux et al.,

TABLE 5 Volumes (voxels) of subcortical regions with unique connections to frontal regions

Structure	Control		bvFTD		p value	Effect size
	M	SD	M	SD		
Striatum						
DLPFC	482	167	322	162	.002	0.961
MPFC	141	64	191	83	.032	0.785
OFC	195	157	117	88	.036	0.498
Thalamus						
DLPFC	391	191	255	181	.020	0.712
MPFC	41	34	89	73	.004	1.400
OFC	43	64	45	69	.927	0.031

Note. Abbreviations: bvFTD = behavioral variant frontotemporal dementia; DLPFC = dorsolateral prefrontal cortex; MPFC = medial prefrontal cortex; OFC = orbitofrontal cortex.

Estimated marginal mean voxels and significance test from separate linear mixed models, controlling for hemisphere, age, gender, education, and intracranial volume.

Note that the relatively large SD of the MPFC and OFC tracts reflects the positively skewed distribution, for which a Gamma-log link function was used.

2015). However, the Bertoux et al. (2015) study was based upon atlas-based segmentation of the striatum and voxel-based analysis, which, in our view, does not account for overlapping regions of connectivity and may have difficulty localizing finer details.

Findings from functional imaging provide support for our results and our interpretation of selective structural hyperconnectivity. Potentially congruent with our findings of selectively increased MPFC connectivity, there has been demonstration of increased functional activity of the default mode network in parallel with decreased salience network activity in bvFTD (Zhou et al., 2010). Given that the default mode network is characteristically anchored in the rostral anterior cingulum/ventral-medial prefrontal cortex, which is included in our MPFC region (Greicius, Krasnow, Reiss, & Menon, 2003), this correlates with our suggestion of increased structural connectivity between MPFC and subcortical structures. Moreover, despite expected reductions in salience network connectivity in bvFTD, Farb et al. (2013) noted MPFC functional hyperconnectivity, which was additionally related to apathy and disinhibition.

Our findings of increased target area volume of the MPFC connections require some consideration of possible underlying cellular changes. In both the basal ganglia and thalamus, cortical representation zones are not clear cut but overlap with neighboring ones (Draganski et al., 2008), which provides a foundation for an expansion of apparent connected volume without resorting to an increased number of axons. Instead, most likely phenomena are increased myelination and/or axonal remodeling/branching of existing neighboring connections, which are plasticity phenomena present in the adult brain known to influence DTI parameters (Zatorre, Fields, & Johansen-Berg, 2012). We propose that the observed increase in MPFC connectivity to striatal and thalamic regions provides structural evidence of this functional hyperconnectivity.

Our findings may shed light on, and be informed by, conditions which have common themes of behavioral dysregulation. Evidence stems from conditions involving hyperconnective MPFC and/or corresponding nodes in subcortical networks, implied either by increased regional size or increased functional connectivity. Structurally, in Parkinson's disease with impulse control disorders, Tessitore et al. (2016) found increased medial prefrontal cortex thickness compared to patients without impulse control disorders. Repetitive behaviors were associated with increased caudate size in persons with autism (Hollander et al., 2005). Furthermore, increased activity in "direct" frontal-striatal-thalamic pathways are noted in obsessive compulsive disorder (Pauls, Abramovitch, Rauch, & Geller, 2014) and unmedicated trichotillomania (Chamberlain et al., 2008). Last, in disorders of addiction, overactivity of the limbic cortical-subcortical loop is thought to be responsible for the compulsivity of this disorder (Volkow & Morales, 2015). In summary, selective hyperfunctioning of frontal circuits are likely involved in multiple pathophysiologic processes which result in behavioral dysregulation (Peters, Dunlop, & Downar, 2016), and particularly compulsive behaviors (Fineberg et al., 2010); these behaviors are signature clinical features of bvFTD.

Despite the findings of consistently altered diffusion metrics across tracts, reduced DLPFC connected region size, and increased MPFC

connected region size, there were few significant correlations observed with behavioral measures. No clear-cut correlation pattern emerged, which may be due to our divisions of cortical and subcortical regions being too specific to capture the more comprehensive FBI scale. Furthermore, from a connectivity perspective, directionality of thalamic-cortical and cortical-thalamic tracts cannot be separated by conventional DTI imaging, and so may have confounded these correlations. Nevertheless, gross severity as measured by the FTLD-CDR-SB was significantly associated with multiple MPFC-striatal tract diffusion metrics, possibly highlighting the importance for this axis in the disease process.

A limitation of our current approach is the *a priori* neuroanatomical and functional tripartite division of the frontal-striatal-thalamic circuits in DLPFC, MPFC, and OFC based projections. This is reasonable since this division is utilized in previous studies investigating the striatum, globus pallidus, thalamus, and in tracts in-between (Behrens et al., 2003; Bertoux et al., 2015; Draganski et al., 2008). Furthermore, we were not able to correct for echo planar imaging distortions, since at the time of study design additional sequences necessary for correction (Smith et al., 2004) were not obtained. Instead, we utilized nonlinear transformations to reduce distortions, and in control participants our pathways and subcortical classification are consistent with previous work (e.g., frontal seed probabilistic tractography in Nakamae et al., 2014) and existing atlases (Behrens et al., 2003; Draganski et al., 2008), suggesting that this methodological limitation was minimized.

5 | CONCLUSION

In conclusion, we have demonstrated that frontal-striatal and frontal-thalamic pathways demonstrate similar altered white matter microstructure, as measured via diffusion tensor imaging metrics, as other previously investigated white matter tracts in bvFTD. Dorsolateral prefrontal cortex connected regions of the dorsal striatum are affected by atrophy as hypothesized in accordance with neuro-pathophysiology underpinned by frontal-striatal and frontal-thalamic circuits. Interestingly, and contrary to our original hypotheses, the medial prefrontal cortex connected regions of the dorsal striatum and thalamus demonstrate significantly increased volume compared to healthy controls. Such increased volumes of connectivity may potentially represent structural evidence of compensatory or maladaptive changes in frontal neuronal network disorder. More broadly, it may indicate deficient top-down modulation, which is a phenomenon that appears common to a range of impulse control disorders.

ACKNOWLEDGMENTS

The authors would like to acknowledge the University of Wollongong's High-Performance Computing cluster for assistance in data processing. Funding for the analysis was provided to DJ by a Miller Family Bridgewater Illawarra Health and Medical Research Initiative Summer Scholarship. JCLL self-funded travel costs and computer infrastructure to coordinate research in Australia and Sweden. The LUPROFS study received funding from The Swedish Alzheimer Foundation, Thuréus Foundation, and benefited from the regional

agreement on medical training and clinical research (ALF) between the Skåne Regional Council and Lund University. Funding for AFS was provided by The Swedish Society for Medical Research and The Bente Rexed Gersteds Foundation for Brain Research. This study was an initiative of the Australian, United States, Scandinavian/Spanish Imaging Exchange network founded and coordinated at the Australian National University Medical School by JCLL. The funders had no role in study design, data collection and analysis, decision to publish, or preparation of the manuscript.

ORCID

David Jakabek  <http://orcid.org/0000-0001-7670-0175>

Jeffrey C. L. Looi  <http://orcid.org/0000-0003-3351-6911>

REFERENCES

- Alexander, G. E., DeLong, M. R., & Strick, P. L. (1986). Parallel organization of functionally segregated circuits linking basal ganglia and cortex. *Annual Review of Neuroscience*, 9(1), 357–381.
- Andersson, J. L. R., Jenkinson, M., & Smith, S. M. (2012). *Non-linear registration aka spatial normalisation (FMRIB Technical Report TR07JA2)*. Oxford, UK: FMRIB Centre. Retrieved from <http://www.fmrib.ox.ac.uk/datasets/techrep/tr07ja2/tr07ja2.pdf>
- Behrens, T. E. J., Johansen-Berg, H., Woolrich, M. W., Smith, S. M., Wheeler-Kingshott, C. A. M., Boulby, P. A., ... Matthews, P. M. (2003). Non-invasive mapping of connections between human thalamus and cortex using diffusion imaging. *Nature Neuroscience*, 6(7), 750–757.
- Bertoux, M., O'Callaghan, C., Flanagan, E., Hodges, J. R., & Hornberger, M. (2015). Fronto-striatal atrophy in behavioral variant frontotemporal dementia and Alzheimer's disease. *Frontiers in Neurology*, 6.
- Bhatia, K. P., & Marsden, C. D. (1994). The behavioural and motor consequences of focal lesions of the basal ganglia in man. *Brain*, 117(4), 859–876.
- Blennow, K., Hampel, H., Weiner, M., & Zetterberg, H. (2010). Cerebrospinal fluid and plasma biomarkers in Alzheimer disease. *Nature Reviews Neurology*, 6(3), 131–144.
- Bohanna, I., Georgiou-Karistianis, N., & Egan, G. F. (2011). Connectivity-based segmentation of the striatum in Huntington's disease: Vulnerability of motor pathways. *Neurobiology of Disease*, 42(3), 475–481.
- Chamberlain, S. R., Menzies, L. A., Fineberg, N. A., del Campo, N., Suckling, J., Craig, K., ... Sahakian, B. J. (2008). Grey matter abnormalities in trichotillomania: Morphometric magnetic resonance imaging study. *British Journal of Psychiatry*, 193(03), 216–221.
- Choi, E. Y., Yeo, B. T. T., & Buckner, R. L. (2012). The organization of the human striatum estimated by intrinsic functional connectivity. *Journal of Neurophysiology*, 108(8), 2242–2263.
- Chow, T. W., Izenberg, A., Binns, M. A., Freedman, M., Stuss, D. T., Scott, C. J. M., ... Black, S. E. (2008). Magnetic resonance imaging in frontotemporal dementia shows subcortical atrophy. *Dementia and Geriatric Cognitive Disorders*, 26(1), 79–88.
- Daianu, M., Mendez, M. F., Baboyan, V. G., Jin, Y., Melrose, R. J., Jimenez, E. E., & Thompson, P. M. (2016). An advanced white matter tract analysis in frontotemporal dementia and early-onset Alzheimer's disease. *Brain Imaging and Behavior*, 10(4), 1038–1053.
- Desikan, R. S., Ségonne, F., Fischl, B., Quinn, B. T., Dickerson, B. C., Blacker, D., ... Killiany, R. J. (2006). An automated labeling system for subdividing the human cerebral cortex on MRI scans into gyral based regions of interest. *NeuroImage*, 31(3), 968–980.
- Draganski, B., Kherif, F., Klöppel, S., Cook, P. A., Alexander, D. C., Parker, G. J. M., ... Frackowiak, R. S. J. (2008). Evidence for segregated and integrative connectivity patterns in the human basal ganglia. *Journal of Neuroscience*, 28(28), 7143–7152.
- Farb, N. A. S., Grady, C. L., Strother, S., Tang-Wai, D. F., Masellis, M., Black, S., ... Chow, T. W. (2013). Abnormal network connectivity in frontotemporal dementia: Evidence for prefrontal isolation. *Cortex*, 49(7), 1856–1873.
- Fineberg, N. A., Potenza, M. N., Chamberlain, S. R., Berlin, H. A., Menzies, L., Bechara, A., ... Hollander, E. (2010). Probing compulsive and impulsive behaviors, from animal models to endophenotypes: A narrative review. *Neuropsychopharmacology*, 35(3), 591–604.
- Forkel, S. J., Thiebaut de Schotten, M., Kawadler, J. M., Dell'Acqua, F., Danek, A., & Catani, M. (2014). The anatomy of fronto-occipital connections from early blunt dissections to contemporary tractography. *Cortex*, 56, 73–84.
- Garibotto, V., Borroni, B., Agosti, C., Premi, E., Alberici, A., Eickhoff, S. B., ... Padovani, A. (2011). Subcortical and deep cortical atrophy in frontotemporal lobar degeneration. *Neurobiology of Aging*, 32(5), 875–884.
- Gordon, E., Rohrer, J. D., & Fox, N. C. (2016). Advances in neuroimaging in frontotemporal dementia. *Journal of Neurochemistry*, 138, 193–210.
- Greicius, M. D., Krasnow, B., Reiss, A. L., & Menon, V. (2003). Functional connectivity in the resting brain: A network analysis of the default mode hypothesis. *Proceedings of the National Academy of Sciences of the United States of America*, 100(1), 253–258.
- Halabi, C., Halabi, A., Dean, D. L., Wang, P.-N., Boxer, A. L., Trojanowski, J. Q., ... Seeley, W. W. (2013). Patterns of striatal degeneration in frontotemporal dementia. *Alzheimer Disease & Associated Disorders*, 27(1), 74–83.
- Hollander, E., Anagnostou, E., Chaplin, W., Esposito, K., Haznedar, M. M., Licalzi, E., ... Buchsbaum, M. (2005). Striatal volume on magnetic resonance imaging and repetitive behaviors in autism. *Biological Psychiatry*, 58(3), 226–232.
- Jang, S. H., & Yeo, S. S. (2014). Thalamocortical connections between the mediodorsal nucleus of the thalamus and prefrontal cortex in the human brain: A diffusion tensor tractographic study. *Yonsei Medical Journal*, 55(3), 709–714.
- Jarbo, K., & Verstynen, T. D. (2015). Converging structural and functional connectivity of orbitofrontal, dorsolateral prefrontal, and posterior parietal cortex in the human striatum. *Journal of Neuroscience*, 35(9), 3865–3878.
- Jbabdi, S., Woolrich, M. W., Andersson, J. L. R., & Behrens, T. E. J. (2007). A Bayesian framework for global tractography. *NeuroImage*, 37(1), 116–129.
- Jones, D. K., & Cercignani, M. (2010). Twenty-five pitfalls in the analysis of diffusion MRI data. *NMR in Biomedicine*, 23(7), 803–820.
- Kertesz, A., Davidson, W., & Fox, H. (1997). Frontal behavioral inventory: Diagnostic criteria for frontal lobe dementia. *Canadian Journal of Neurological Sciences/Journal Canadien Des Sciences Neurologiques*, 24(01), 29–36.
- Klein, J. C., Rushworth, M. F. S., Behrens, T. E. J., Mackay, C. E., de Crespigny, A. J., D'Arceuil, H., & Johansen-Berg, H. (2010). Topography of connections between human prefrontal cortex and mediodorsal thalamus studied with diffusion tractography. *NeuroImage*, 51(2), 555–564.
- Knopman, D. S., Kramer, J. H., Boeve, B. F., Caselli, R. J., Graff-Radford, N. R., Mendez, M. F., ... Mercaldo, N. (2008). Development of methodology for conducting clinical trials in frontotemporal lobar degeneration. *Brain*, 131(11), 2957–2968.
- Landin-Romero, R., Kumfor, F., Leyton, C. E., Irish, M., Hodges, J. R., & Piguet, O. (2016). Disease-specific patterns of cortical and subcortical

- degeneration in a longitudinal study of Alzheimer's disease and behavioural-variant frontotemporal dementia. *NeuroImage*.
- Leemans, A., & Jones, D. K. (2009). The B-matrix must be rotated when correcting for subject motion in DTI data. *Magnetic Resonance in Medicine*, 61(6), 1336–1349.
- Looi, J. C. L., Lindberg, O., Liberg, B., Tatham, V., Kumar, R., Maller, J., ... Wahlund, L.-O. (2008). Volumetrics of the caudate nucleus: Reliability and validity of a new manual tracing protocol. *Psychiatry Research*, 163(3), 279–288.
- Looi, J. C. L., Svensson, L., Lindberg, O., Zandbelt, B. B., Ostberg, P., Orndahl, E., & Wahlund, L.-O. (2009). Putaminal volume in frontotemporal lobar degeneration and Alzheimer disease: Differential volumes in dementia subtypes and controls. *American Journal of Neuroradiology*, 30(8), 1552–1560.
- Looi, J. C. L., & Walterfang, M. (2013). Striatal morphology as a biomarker in neurodegenerative disease. *Molecular Psychiatry*, 18(4), 417–424.
- Looi, J. C. L., Walterfang, M., Velakoulis, D., Macfarlane, M. D., Svensson, L. A., & Wahlund, L.-O. (2012). Frontotemporal dementia as a frontostriatal disorder: Neostriatal morphology as a biomarker and structural basis for an endophenotype. *Australian & New Zealand Journal of Psychiatry*, 46(5), 422–434.
- Macfarlane, M. D., Jakabek, D., Walterfang, M., Vestberg, S., Velakoulis, D., Wilkes, F. A., ... Santillo, A. F. (2015). Striatal atrophy in the behavioural variant of frontotemporal dementia: Correlation with diagnosis, negative symptoms and disease severity. *PLoS ONE*, 10(6), e0129692.
- Mackenzie, I. R. A., & Neumann, M. (2016). Molecular neuropathology of frontotemporal dementia: Insights into disease mechanisms from postmortem studies. *Journal of Neurochemistry*, 138, 54–70.
- Mahoney, C. J., Ridgway, G. R., Malone, I. B., Downey, L. E., Beck, J., Kinnunen, K. M., ... Warren, J. D. (2014). Profiles of white matter tract pathology in frontotemporal dementia. *Human Brain Mapping*, 35(8), 4163–4179.
- Möller, C., Hafkemeijer, A., Pijnenburg, Y. A. L., Rombouts, S. A. R. B., van der Grond, J., Doppler, E., ... van der Flier, W. M. (2015). Joint assessment of white matter integrity, cortical and subcortical atrophy to distinguish AD from behavioral variant FTD: A two-center study. *NeuroImage: Clinical*, 9, 418–429.
- Nakamae, T., Sakai, Y., Abe, Y., Nishida, S., Fukui, K., Yamada, K., ... Narumoto, J. (2014). Altered fronto-striatal fiber topography and connectivity in obsessive-compulsive disorder. *PLoS ONE*, 9(11), e112075.
- O'Callaghan, C., Bertoux, M., & Hornberger, M. (2014). Beyond and below the cortex: The contribution of striatal dysfunction to cognition and behaviour in neurodegeneration. *Journal of Neurology, Neurosurgery, and Psychiatry*, 85(4), 371–378.
- Pauls, D. L., Abramovitch, A., Rauch, S. L., & Geller, D. A. (2014). Obsessive-compulsive disorder: An integrative genetic and neurobiological perspective. *Nature Reviews Neuroscience*, 15(6), 410–424.
- Peters, S. K., Dunlop, K., & Downar, J. (2016). Cortico-striatal-thalamic loop circuits of the salience network: A central pathway in psychiatric disease and treatment. *Frontiers in Systems Neuroscience*, 10.
- Petrides, M., & Pandya, D. N. (2002). Comparative cytoarchitectonic analysis of the human and the macaque ventrolateral prefrontal cortex and corticocortical connection patterns in the monkey. *European Journal of Neuroscience*, 16(2), 291–310.
- Piguet, O., Hornberger, M., Mioshi, E., & Hodges, J. R. (2011). Behavioural-variant frontotemporal dementia: Diagnosis, clinical staging, and management. *Lancet. Neurology*, 10(2), 162–172.
- Piray, P., Toni, I., & Cools, R. (2016). Human choice strategy varies with anatomical projections from ventromedial prefrontal cortex to medial striatum. *Journal of Neuroscience*, 36(10), 2857–2867.
- Power, B. D., Wilkes, F. A., Hunter-Dickson, M., van Westen, D., Santillo, A. F., Walterfang, M. ... (2015). Validation of a protocol for manual segmentation of the thalamus on magnetic resonance imaging scans. *Psychiatry Research*, 232(1), 98–105.
- Rascovsky, K., Hodges, J. R., Knopman, D., Mendez, M. F., Kramer, J. H., Neuhaus, J., ... Miller, B. L. (2011). Sensitivity of revised diagnostic criteria for the behavioural variant of frontotemporal dementia. *Brain*, 134(9), 2456–2477.
- Santillo, A. F., Lundblad, K., Nilsson, M., Landqvist Waldö, M., van Westen, D., Lätt, J., ... Nilsson, C. (2016). Grey and white matter clinico-anatomical correlates of disinhibition in neurodegenerative disease. *PLoS ONE*, 11(10), e0164122.
- Santillo, A. F., Mårtensson, J., Lindberg, O., Nilsson, M., Manzouri, A., Landqvist Waldö, M., ... Nilsson, C. (2013). Diffusion tensor tractography versus volumetric imaging in the diagnosis of behavioral variant frontotemporal dementia. *PLoS ONE*, 8(7), e66932.
- Schmahmann, J., & Pandya, D. (2009). *Fiber pathways of the brain* (1st ed.). Oxford: Oxford University Press.
- Schroeter, M. L., Laird, A. R., Chwiesko, C., Deuschl, C., Schneider, E., Bzdok, D., ... Neumann, J. (2014). Conceptualizing neuropsychiatric diseases with multimodal data-driven meta-analyses - the case of behavioral variant frontotemporal dementia. *Cortex*, 57, 22–37.
- Schroeter, M. L., Raczka, K., Neumann, J., & von Cramon, D. Y. (2008). Neural networks in frontotemporal dementia—a meta-analysis. *Neurobiology of Aging*, 29(3), 418–426.
- Seeley, W. W., Crawford, R. K., Zhou, J., Miller, B. L., & Greicius, M. D. (2009). Neurodegenerative diseases target large-scale human brain networks. *Neuron*, 62(1), 42–52.
- Smith, S. M., Jenkinson, M., Woolrich, M. W., Beckmann, C. F., Behrens, T. E. J., Johansen-Berg, H., ... Matthews, P. M. (2004). Advances in functional and structural MR image analysis and implementation as FSL. *NeuroImage*, 23, S208–S219.
- Tessitore, A., Santangelo, G., De Micco, R., Vitale, C., Giordano, A., Raimo, S., ... Tedeschi, G. (2016). Cortical thickness changes in patients with Parkinson's disease and impulse control disorders. *Parkinsonism & Related Disorders*, 24, 119–125.
- Tziortzi, A. C., Haber, S. N., Searle, G. E., Tsoumpas, C., Long, C. J., Sholtz, P., ... Gunn, R. N. (2013). Connectivity-based functional analysis of dopamine release in the striatum using diffusion-weighted MRI and positron emission tomography. *Cerebral Cortex*, bhs397.
- Volkow, N. D., & Morales, M. (2015). The brain on drugs: From reward to addiction. *Cell*, 162(4), 712–725.
- Woolrich, M. W., Jbabdi, S., Patenaude, B., Chappell, M., Makni, S., Behrens, T., ... Smith, S. M. (2009). Bayesian analysis of neuroimaging data in FSL. *NeuroImage*, 45(1), S173–S186.
- Yushkevich, P. A., Piven, J., Hazlett, H. C., Smith, R. G., Ho, S., Gee, J. C., & Gerig, G. (2006). User-guided 3D active contour segmentation of anatomical structures: Significantly improved efficiency and reliability. *NeuroImage*, 31(3), 1116–1128.
- Zatorre, R. J., Fields, R. D., & Johansen-Berg, H. (2012). Plasticity in gray and white: Neuroimaging changes in brain structure during learning. *Nature Neuroscience*, 15(4), 528–536.
- Zhang, H., Schneider, T., Wheeler-Kingshott, C. A., & Alexander, D. C. (2012). NODDI: Practical in vivo neurite orientation dispersion and density imaging of the human brain. *NeuroImage*, 61(4), 1000–1016.
- Zhang, Y., Schuff, N., Du, A.-T., Rosen, H. J., Kramer, J. H., Gorno-Tempini, M. L., ... Weiner, M. W. (2009). White matter damage in frontotemporal dementia and Alzheimer's disease measured by diffusion MRI. *Brain*, 132(9), 2579–2592.

Zhou, J., Greicius, M. D., Gennatas, E. D., Growdon, M. E., Jang, J. Y., Rabinovici, G. D., ... Seeley, W. W. (2010). Divergent network connectivity changes in behavioural variant frontotemporal dementia and Alzheimer's disease. *Brain*, 133(5), 1352–1367.

SUPPORTING INFORMATION

Additional Supporting Information may be found online in the supporting information tab for this article.

How to cite this article: Jakabek D, Power BD, Macfarlane MD, et al. Regional structural hypo- and hyperconnectivity of frontal-striatal and frontal-thalamic pathways in behavioral variant frontotemporal dementia. *Hum Brain Mapp.* 2018;39:4083–4093. <https://doi.org/10.1002/hbm.24233>